Dynamic features of brain edema in rat models of traumatic brain injury

Huanhuan Ren and Hong Lu

We explored the dynamic features of brain edema after traumatic brain injury (TBI) using healthy adult male Wistar rats. After inducing moderate brain injuries in the rats, we divided them randomly among seven groups on the basis of the time elapsed between TBI and examination: 1, 6, 12, 24, 48, 72, and 168 h. All rats were scanned using diffusion-weighted imaging (DWI) to observe tissue changes in the contusion penumbra (CP) after TBI. Immunoglobulin G expression was also detected. At 1 h after TBI, there was an annular light-colored region in the CP where the intercellular space was enlarged, suggesting vasogenic edema. At 6 h, the cells expanded, their nuclei shrank, and the cytoplasm was replaced by vacuoles, indicating intracellular edema. Vasogenic edema and intracellular edema increased 12 h after TBI, but decreased 24 h after TBI, with vasogenic edema increasing 48 h after TBI. By 72 h after TBI, intracellular edema dominated until resolution of all edema by 168 h after TBI. DWI indicated that the relative apparent diffusion coefficient increased markedly at 1 h after TBI, but was reduced at 6 and 12 h after TBI. At 48 h, relative apparent diffusion coefficient increased gradually and then declined at 72 h. In rats, TBI-related changes include dynamic variations in intracellular and vasogenic edema severity. Routine MRI and DWI examinations do not distinguish between the center of trauma and CP; however, the apparent diffusion coefficient diagram can portray variations in CP edema type and degree at different time-points following TBI. *NeuroReport* 30:605–611 Copyright © 2019 The Author(s). Published by Wolters Kluwer Health, Inc.

Department of Radiology, Chongqing Seventh People's Hospital, Chongqing, China

Correspondence to Hong Lu, PhD, Department of Radiology, Chongqing Seventh People's Hospital, Chongqing 400054, China
Tel/fax: + 86 023 6286 8902; e-mail: cqlh@sohu.com

Introduction

Millions of individuals sustain traumatic brain injury (TBI) every year. In addition to direct structural injury, TBI can also activate neural inflammatory signaling and induce brain edema by breaking the blood–brain barrier. Cytotoxic edema and vasogenic edema resulting from TBI eventually lead to neuronal death [1]. TBI accounts for one-third of all trauma-induced injuries, and it is predicted by the WHO that TBI will likely remain a predominant cause of death and disability until 2020 [2].

Clinical treatment for TBI is limited because the pathological changes occurring after TBI are not well understood. However, neuroimaging can help predict secondary injury following TBI and may be used to diagnose neurological diseases through the assessment of reliable biomarkers. Thus, neuroimaging provides information that aids clinicians in accurate TBI prognosis [3]. MRI provides high-resolution images of soft tissues. Routine MRI examinations, such as T1-weighted image (WI) and T2-WI, can provide basic anatomic information and some physiological information. As a complementary means, fluid-attenuated inversion recovery (FLAIR) can achieve clearer imaging of the cortex and cerebral ventricles by suppressing the influence of cerebrospinal fluid. However, these methods cannot distinguish types of edema at the center and contusion penumbra (CP) of trauma sites because intracellular and vasogenic edema show as equivalent signals in T1-WI, T2-WI, and T2FLAIR images. Intracellular and vasogenic edema manifest as medium and low-strength signals in T1WI images and as high-strength signals in T2-WI and T2FLAIR images. Diffusion-weighted imaging (DWI) can reflect the motility of water molecules, whereas the apparent diffusion coefficient (ADC) can be used to analyze water diffusion quantitatively. The magnitude of the ADC directly reflects the level of water molecule motion. The type of edema occurring after TBI can be determined using DWI [4]. Intracellular edema has a lower ADC because of excessive water aggregation and weaker mobility of water molecules in cells [5]. In contrast, vasogenic edema has a comparatively higher ADC because in such cases, water molecules enter the brain parenchyma through the broken blood–brain barrier and distribute abnormally in the interstices, after which the intercellular space enlarges, allowing water molecules to move freely. We investigated edema changes at the center of trauma in previous experiments, which showed that the type and degree of edema changed continuously [6].

During TBI, injury occurs at the periphery in addition to a series of pathological changes at the area subjected to direct

injury (center of trauma). For example, an ischemia penumbra (IP) is formed around the injury focus after acute ischemia. Similarly, a CP may occur after TBI. In comparison with the center of trauma, tissue injury in the CP is less serious, whereas tissue necrosis is incomplete. Therefore, it is possible to repair the tissue at the CP. Following the assessment of edema in the CP, the development of edema can be prevented, whereas intracranial hypertension and secondary clinical symptoms can be relieved. In this study, edema was assessed in the CP at different time-points following TBI in rats. The ADC was calculated to characterize changes in edema type and degree for the purpose of providing reliable imaging analysis sufficient to guide patient treatment.

Materials and methods
Experimental animals and grouping
Forty-nine adult male Wistar rates (250 g each) were purchased from the Laboratory Animal Center of Sichuan University (Chengdu, China; license no. SCXKZ|2013-24). The rats were housed in a facility under a 12 h light and 12 h dark cycle and temperature of 22–25°C, with free access to water and food. Using a random number table, the rats were divided into seven groups of seven rats each on the basis of the time-point after TBI at which they were assessed: 1, 6, 12, 24, 48, 72, and 168 h. All rats received an initial MRI scan, after which six rats were selected from each group. Hematoxylin and eosin (H&E) staining and immunoglobulin (Ig) G assays were performed on brain tissue from the selected rats to observe pathological changes in tissues and detect IgG expression in the CP. The brain tissue of the remaining rat in each group was observed under an electron microscope.

Establishment of animal models
By referring to the improved Feeney's method, moderate brain injury was modeled using a PinPoint Precision Cortical Impactor (Hatteras Instruments, Cary, North Carolina, USA). Each rat was first narcotized by an intraperitoneal injection of 1% pentobarbital sodium (0.4 ml/100 g), after which an incision of ~2.0 cm was made on the scalp along the median line. A dental bench drilling machine (model: 307-2B; Shanghai Lingzhiqi Precision Tool Ltd, Shanghai, China) and a drill with a diameter of 1.5 mm were used to drill a hole in the skull 2.5 mm behind the bregma and 2.5 mm to the right of the sagittal line. The hole was then expanded by mosquito clamp to produce a bone window with a diameter of ~4 mm. After fixing the head of each rat in the stereotaxic apparatus (ST-7; Narishige, Tokyo, Japan), its brain was impacted to produce moderate brain injury. The impact parameters were selected according to the results of a previous experiment [7]: impact velocity, 2.5 m/s; impact depth, 4.0 mm; impact duration, 85 ms; and diameter of the impactor head, 4 mm.

MRI examination
All rats were narcotized by an intraperitoneal injection of 1% pentobarbital sodium (0.4 ml/100 g) and implanted with a phased-array coil intended for use in laboratory animals (Shanghai Chenguang Medical Technologies Co. Ltd). Each rat was laid on its back and scanned using a 3.0-T MRI scanner (Signa HDx; GE Healthcare, Chicago, Illinois, USA) with the optic chiasma as the center of the field. The DWI parameters were as follows: TR, 3000 ms; TE, 72.6 ms; $b = 0 \text{ s/mm}^2$ and 800 s/mm^2; and NEX = 12. After scanning, all images were transmitted to an AWD4.3 workstation and processed using Functool.

Image processing and analysis
ADC diagrams were generated following image processing by Functool, after which regions of interest (ROIs) were demarcated in the CP. The ADC was expressed as a relative apparent diffusion coefficient value [rADC; rADC (%) = ADC value of the ROI on the side of injury/ADC value of the ROI in the corresponding region in the contralateral uninjured side of the brain × 100]. At least two experienced physicians with no knowledge of the experimental design or expected test outcomes measured each ROI. Hemorrhagic foci were avoided when selecting ROIs. To ensure precise positioning, ROIs were selected and measured on the basis of pathology [8].

Pathomorphological observation by a light microscope and a transmission electron microscope
Six rats from each group were first narcotized by an intraperitoneal injection of 1% pentobarbital sodium (0.4 ml/100 g). The rats were decapitated, after which the brain of each rat was collected and fixed in 150 ml of 4% paraformaldehyde solution. After routine paraffin embedding, each brain was sliced and subjected to routine H&E staining. Each stained tissue section was observed under a light microscope and photographed.

One rat from each group was killed by an intraperitoneal injection of 2 ml of 10% chloral hydrate (0.4 ml/100 g). The tissue (1 mm × 1 mm × 1 mm) around the injury was collected and placed immediately in a 2.5% glutaraldehyde solution. The tissue was fixed in 10 g/l osmium tetroxide, dehydrated in a series of acetone solutions, embedded in Epon812, sectioned, and stained with dyes containing lead and uranium. Finally, the cellular structure and subcellular fractions were observed.

Immunoglobulin G immunohistochemical staining of brain tissue
The brain tissue sections subjected to H&E staining were used for the immunohistochemical detection of IgG. Four sections from each rat were assessed. Five visual fields of each section were observed, and the positive cells under each visual field were counted. A coronal section was made at the layer in which the most serious injury was observed. IgG immunohistochemical staining was carried out using the two-step EnVision color developing technique (GLK500705; Agilent Technologies, Inc., Santa Clara, California, USA). Each paraffin-embedded section was dewaxed, hydrated, incubated in H_2O_2, and rinsed three

times with PBS, after which primary antibodies against IgG (1 : 8000) (Santa Cruz Biotechnology, Santa Cruz, California, USA) were added dropwise. After an overnight incubation at 4°C, each section was rinsed three times with PBS and exposed to IgG (1 : 500) (Santa Cruz Biotechnology) for 20 min at room temperature, after which the section was rinsed three times with PBS and exposed to DAB solution. Color development was stopped immediately when it was observed under a light microscope, after which the section was mounted. The IgG immunohistochemistry results were graded using the method of Akiguchi *et al.* [9].

Statistical analysis

All data are expressed as mean ± SD and were analyzed by one-way analysis of variance and the least significant difference method using SPSS 20.0 (IBM Corp., Armonk, New York, USA). The threshold of statistical significance was P value less than 0.05.

Results
MRI examination

The ADC showed an inconsistent variation in the center of trauma and its periphery. In the surrounding CP, the rADC increased markedly at 1 h after TBI, decreased at 6 h after TBI, and plateaued at 12 and 24 h after TBI. The rADC increased again at 48 h after TBI and declined at 72 h after TBI, after which it tended to be normal until 168 h after TBI, but remained lower than that of the control group (Figs 1 and 2).

Structural changes in the contusion penumbra following traumatic brain injury

No abnormal changes were observed in the control group. At 1 h after injury, a light-colored edema zone occurred in the CP, whereas larger gaps between blood vessels were observed, indicating vasogenic edema. Electron microscopy indicated that the blood–brain barrier had a discontinuous basement membrane with a rough edge. At 6 h after TBI, gliocytes in the CP swelled, whereas intracellular vacuolar degeneration and narrowing of the intercellular spaces were

observed, suggesting intracellular edema. In addition, swollen organelles and the rupture and disappearance of mitochondrial cristae were observed by electron microscopy. At 12 h after TBI, intracellular edema and vasogenic edema were aggravated, whereas large areas of vacuole-like cells and light-colored latticed intercellular substance were observed by electron microscopy. At 24 h after TBI, intracellular edema and vasogenic edema were alleviated, but vasogenic edema was aggravated again until 48 h after TBI. At 72 h after TBI, electron microscopy showed that the number of swollen gliocytes was increased, whereas intracellular edema was the predominant form of edema. Intracellular edema and vasogenic edema were alleviated at 168 h after TBI (Figs 3 and 4).

Semiquantitative immunohistochemical detection of immunoglobulin G expression

In the immunohistochemical experiments, the staining intensity was associated directly with IgG expression and the severity of damage to the blood–brain barrier. IgG immunostaining was strongly positive (+ + +) at 1, 12,

Fig. 2
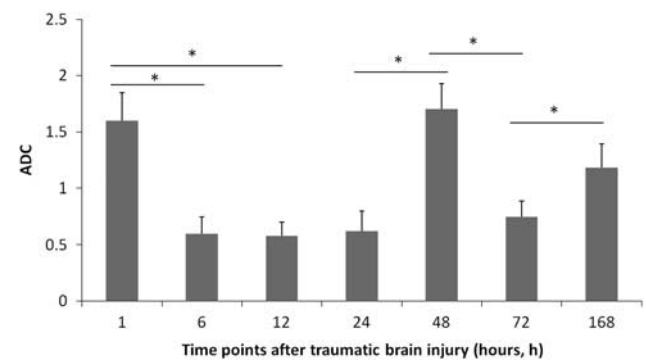
Quantification of apparent diffusion coefficient (ADC) variation in the contusion penumbra at different time-points after traumatic brain injury. One-way analysis of variance indicated that the differences between all pairs of time-points were significant ($P < 0.05$), except for those between the 6 and 12 h ($P = 0.196$), 6 and 24 h ($P = 0.862$), and 12 and 24 h time-points ($P = 0.144$). *Differences between two pairs of time-points were significant ($P < 0.05$).
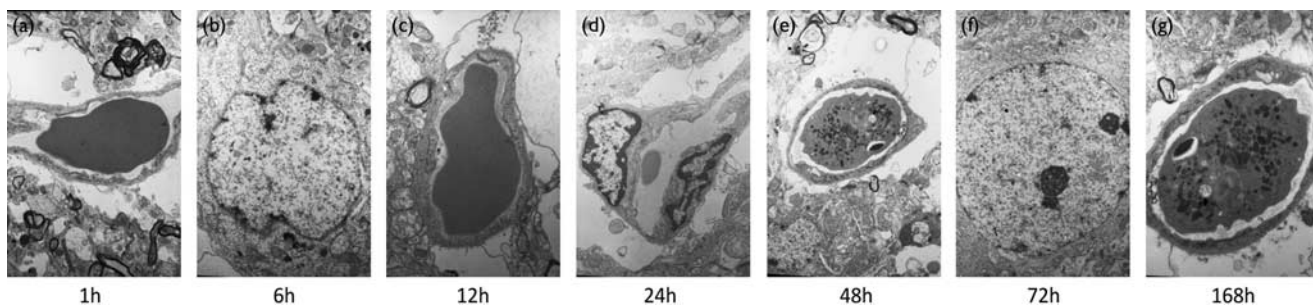
Fig. 1
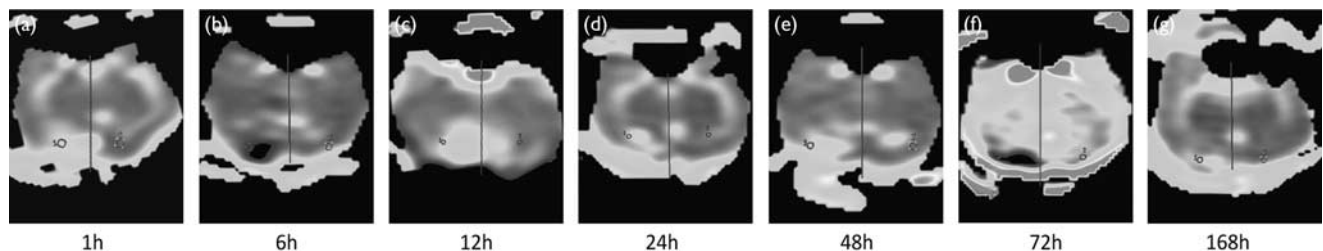
Apparent diffusion coefficient variation in the contusion penumbra at different time-points after traumatic brain injury. (a–g) The apparent diffusion coefficient at 1, 6, 12, 24, 48, 72, and 168 h after traumatic brain injury. '1' indicates a region of interest in the periphery of trauma (i.e. the contusion penumbra), whereas '2' indicates the region contralateral to the damaged side.
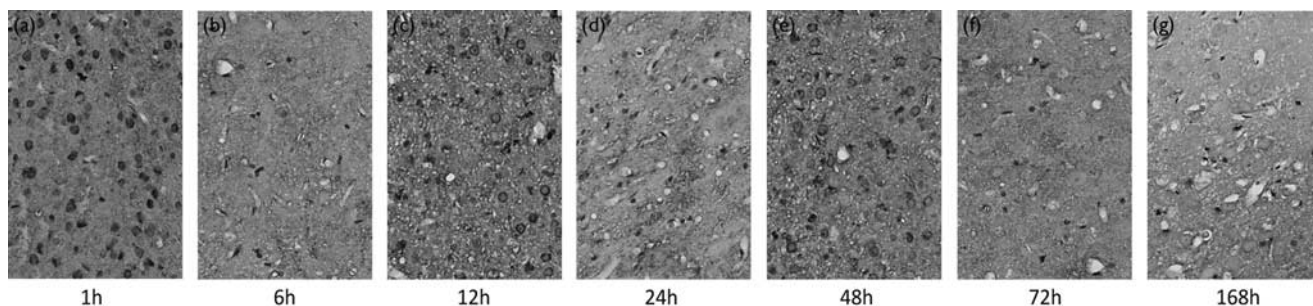
Fig. 3
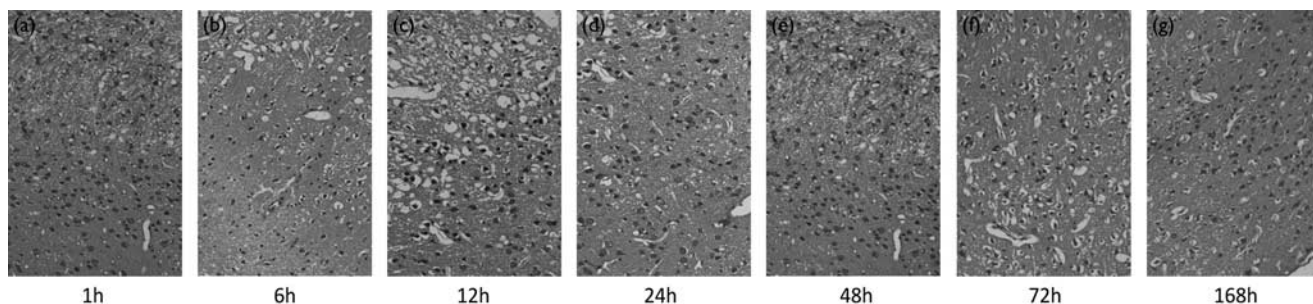
Microstructural changes associated with edema in the contusion penumbra at different time-points after traumatic brain injury. (a–g) The variations in brain edema at 1, 6, 12, 24, 48, 72, and 168 h after traumatic brain injury (hematoxylin and eosin staining, ×100 magnification).

Fig. 4

Ultrastructural changes associated with edema in the contusion penumbra at different time-points after traumatic brain injury. (a–g) The variations in brain edema at 1, 6, 12, 24, 48, 72, and 168 h after traumatic brain injury (transmission electron microscope).

Fig. 5

Immunoglobulin G expression in the contusion penumbra at different time-points after traumatic brain injury. (a–g) The variations in brain edema at 1, 6, 12, 24, 48, 72, and 168 h after traumatic brain injury (immunohistochemical staining).

and 48 h after TBI, indicating that the BBB was damaged considerably and its permeability was increased markedly. IgG immunostaining was weakly positive (+) at 6, 24, 72, and 168 h after TBI, indicating less damage to the blood–brain barrier at these time-points in comparison with that observed at earlier time-points (Fig. 5).

Discussion

The dynamic pathological changes occurring after TBI necessitate reliance on neuroimaging for accurate prognoses [10]. Neuroimaging can identify recoverable regions, for example, the CP, and provide information facilitating accurate clinical prognosis and effective

treatment [3]. It has been reported that the sex hormones of female animals, especially progesterone, can relieve edema after TBI [11]. Therefore, we used male rats in our study to exclude hormonal interference.

TBI consists of direct and secondary injury, and the latter may result in serious intracranial hypertension and reduced cerebral perfusion [12,13]. The major pathological change after TBI is brain edema consisting of vasogenic and intracellular edema [14]. Vasogenic edema is attributed to the entrance of water and plasma proteins into the interstitial space because of damage to the blood–brain barrier. Intracellular edema is a result of mitochondrial swelling and disturbed ATP generation after excessive water influx into cells [14]. Moreover, reduced cerebral blood flow (CBF) interferes with ion movement and aggravates intracellular edema. This edema cycle generally does not stop until death and can lead to permanent injury [15]. Studies on post-TBI pathological changes in the center of trauma have led some scholars to report that vasogenic edema is predominant in the center of trauma [16], whereas others argue that intracellular edema is predominant in this region [17,18]. However, post-TBI pathological changes in the periphery of trauma have seldom been studied.

Knowledge on contusion penumbra
An IP comprised of active injured tissue is formed after ischemic cerebral injury. CBF is reduced in the IP, but it does not reach the threshold that can cause irreversible cell membrane dysfunction [19]. Similarly, an annular region around the center of trauma comprises a transition zone between central injured tissue and peripheral normal tissue, where tissue is injured, but not necrotic. Pathologically, the CP presents tissue edema following TBI [11,20]. The CBF in the penumbra is sufficient to maintain morphologic integrity, but lower than that required to maintain tissue function. Brain tissue in the penumbra can achieve normal functioning following timely and effective intervention after TBI; therefore, such tissue has been considered a target area of clinical treatment [21].

Detection of edema in the contusion penumbra and its significance
We found that both the degree and the type of edema in the CP changed with time after TBI. Edema appeared at 1 h, was slightly aggravated at 6 h, and became most severe at 12 h. H&E staining showed that intracellular and vasogenic edema were predominant in the CP at 1 and 6 h after TBI, respectively; both types of edema were significantly aggravated at 12 h and then relieved.

IgG expression was used as an indirect indicator of the degree of damage to the blood–brain barrier, with increased IgG expression indicative of vasogenic edema [22]. Detection of blood–brain barrier permeability facilitates accurate clinical prognosis [23]. Strong positive (+++) expression of IgG at 1, 12, and 48 h suggests remarkable breakdown of the blood–brain barrier and vasogenic edema. The relatively weaker IgG signal observed at other time-points indicated alleviation of vasogenic edema. The blood–brain barrier is the major protective barrier of the brain [24]. It is believed that the blood–brain barrier is not disturbed in a single episode; instead, the blood–brain barrier is impaired first during the early stage after TBI, followed by another episode of impaired functioning later in the progression of the injury [25]. Our experiments also indicated that blood–brain barrier impairment occurred in two distinct stages, but this idea remains controversial [26].

Distinction of edema type can help clinicians assess disease [8]. An analysis of the correlation between TBI prognosis and edema type found that brain edema is an important influence on prognosis [4]. Galloway et al. [27] found that tissue subjected to intracellular edema had a poor prognosis. In the case of intracellular edema, mitochondrial dysfunction leads to failure to produce sufficient energy, resulting in irreversible cell death. However, vasogenic edema may be reversible [28].

Contusion penumbra demarcation by the apparent diffusion coefficient diagram
Following TBI, the center of trauma and CP show distinct and diverse pathological changes [14]. The ADC varies with the particular pathology of each TBI. It has been reported that the ADC usually increased in the injury area during the early stage of damage following TBI [29], but other studies have found that the ADC was decreased in the injury area during this time [30]. There is controversy on which type of edema is predominant after TBI. Some studies have reported that vasogenic edema increases the ADC [10], whereas intracellular edema reduces the ADC [31]. Moreover, some studies have found that both intracellular edema and vasogenic edema occur after TBI [25]. This controversy may be attributed to differences in established trauma models and MRI methods, as well as the failure to classify injury and its degree [5].

Significant research has been performed to study the center of trauma, but few studies have assessed ADC changes in the CP. In the ADC diagram, the center of trauma and CP showed differing signal intensity and the ADC varied markedly with time. The rADC in the CP was slightly increased at 1 h, indicating that vasogenic edema was the primary type of edema occurring at this time-point. Because the rADC reflects the combined effects of two types of edema, the existence of intracellular edema at 1 h after TBI cannot be excluded (vasogenic and intracellular edema coexisted and the former dominated at 1 h). The rADC began to decrease at 6 h after TBI, suggesting that intracellular edema dominated at this time-point. The rADC was low at 12 and 24 h after TBI, but the degree of edema was inconsistent.

Both types of edema were more severe at 12 h after TBI than at 6 h after TBI, but were alleviated at 24 h after TBI. The rADC difference was not prominent because of the combined effect of both types of edema. At 48 h after TBI, the rADC was obviously increased, suggesting the predominance of vasogenic edema. At 72 h after TBI, intracellular edema was slightly aggravated, leading to a decrease in the rADC. At 168 h after TBI, the rADC was increased slightly. The results described above indicate that changes in the ADC diagram can allow clinicians to distinguish between the center of trauma and CP by reflecting pathological changes in the CP. Moreover, our results show that the difference in the ADC of the CP after TBI is mainly caused by the coexistence of intracellular and extracellular edema.

The difference in the type of edema occurring in the injury area and CP has been recognized in a similar study [25], which showed that the injury area was mainly subjected to intracellular edema, whereas the periphery was mainly affected by vasogenic edema [25]. No consensus has been reached on which type of edema is the main pathological change in the CP after TBI [32]. The ADC in the injury area was increased 6 h after TBI, but it declined in the periphery [33]. The increase in the ADC in the center of trauma corresponded to necrosis, whereas the decrease in the ADC in the periphery was attributed to shrinking of the intercellular space after cellular edema [33]. The CP was defined by diffusion tensor imaging as the area subjected to intracellular edema and with low ADC in the periphery of trauma [34].

Wei *et al.* [25] argued that the periphery of trauma can be recognized using T2WI, in which a strong signal indicates the injury area, whereas the surrounding normal area is the periphery. Although many experiments have found that a strong T2 signal after stroke usually represents a reversible injury [35], the idea that the CP can be determined by the T2 diagram remains controversial [36]. Some experiments indicate that tissue injury might be reversible when the signal was abnormal in DWI, but normal in T2 imaging [37], but this condition was not assessed in our study.

Conclusion
A CP occurs around the center of trauma after TBI, in which the major pathological change is dynamic alternation of edema of varying degree and type. DWI to assess ADC is capable of distinguishing between the center of trauma and the CP. In addition, the ADC diagram can also clearly display the type and degree of edema at different time-points following TBI, providing valuable image information for clinicians on patient treatment.

Acknowledgements

Conflicts of interest
There are no conflicts of interest.

References
1　Schmidt OI, Heyde CE, Ertel W, Stahel PF. Closed head injury – an inflammatory disease? *Brain Res Brain Res Rev* 2005; **48**:388–399.
2　Mcintosh TK, Juhler M, Wieloch T. Novel pharmacologic strategies in the treatment of experimental traumatic brain injury: 1998. *J Neurotrauma* 1998; **15**:731–769.
3　Mechtler LL, Shastri KK, Crutchfield KE. Advanced neuroimaging of mild traumatic brain injury. *Neurol Clin* 2014; **32**:31–58.
4　Donkin JJ, Vink R. Mechanisms of cerebral edema in traumatic brain injury: therapeutic developments. *Curr Opin Neurol* 2010; **23**:293–299.
5　Prieto-Valderrey F, Muñiz-Montes JR, López-García JA, Villegas-Del OJ, Málaga-Gil J, Galván-García R. Utility of diffusion-weighted magnetic resonance imaging in severe focal traumatic brain injuries. *Med Intensiva* 2013; **37**:375–382.
6　Zhang C, Chen J, Lu H. Expression of aquaporin-4 and pathological characteristics of brain injury in a rat model of traumatic brain injury. *Mol Med Rep* 2015; **12**:7351–7357.
7　Chen JQ, Zhang CC, Lu H, Wang W. Assessment of traumatic brain injury degree in animal model. *Asian Pac J Trop Med* 2014; **7**:991–995.
8　Maegele M, Stuermer EK, Hoeffgen A, Uhlenkueken U, Mautes A, Schaefer N, et al. Multimodal MR imaging of acute and subacute experimental traumatic brain injury: time course and correlation with cerebral energy metabolites. *Acta Radiol Short Rep* 2015; **4**:2047981614555142.
9　Akiguchi I, Tomimoto H, Suenaga T, Wakita H, Budka H. Blood–brain barrier dysfunction in Binswanger's disease; an immunohistochemical study. *Acta Neuropathol* 1997; **95**:78–84.
10　Pasco A, Lemaire L, Franconi F, Lefur Y, Noury F, Saint-André JP, et al. Perfusional deficit and the dynamics of cerebral edemas in experimental traumatic brain injury using perfusion and diffusion-weighted magnetic resonance imaging. *J Neurotrauma* 2007; **24**:1321–1330.
11　O'Connor CA, Cernak I, Vink R. *The temporal profile of edema formation differs between male and female rats following diffuse traumatic brain injury*. Vienna, Austria: Springer; 2006.
12　Le TH, Gean AD. Neuroimaging of traumatic brain injury. *Mt Sinai J* 2010; **76**:145–162.
13　Gaddam SS, Buell T, Robertson CS. Systemic manifestations of traumatic brain injury. *Handb Clin Neurol* 2015; **127**:205–218.
14　Lescot T, Fullaoller L, Fullaoller L, Po C, Chen XR, Puybasset L, et al. Temporal and regional changes after focal traumatic brain injury. *J Neurotrauma* 2010; **27**:85–94.
15　McBride DW, Szu JI, Hale C, Hsu MS, Rodgers VG, Binder DK. Reduction of cerebral edema after traumatic brain injury using an osmotic transport device. *J Neurotrauma* 2014; **31**:1948–1954.
16　Zlokovic BV. The blood–brain barrier in health and chronic neurodegenerative disorders. *Neuron* 2008; **57**:178–201.
17　Gasparetto EL, Lopes FCR, Domingues RC, Domingues RC. Diffusion imaging in traumatic brain injury. *Neuroimaging Clin N Am* 2011; **21**:115–125.
18　Blixt J, Svensson M, Gunnarson E, Wanecek M. Aquaporins and blood–brain barrier permeability in early edema development after traumatic brain injury. *Brain Res* 2015; **1611**:18–28.
19　Astrup J, Siesjö BK, Symon L. Thresholds in cerebral ischemia – the ischemic penumbra. *Stroke* 1981; **12**:723–725.
20　Harish G, Mahadevan A, Pruthi N, Sreenivasamurthy SK, Puttamallesh VN, Keshava Prasad TS, et al. Characterization of traumatic brain injury in human brains reveals distinct cellular and molecular changes in contusion and pericontusion. *J Neurochem* 2015; **134**:156–172.
21　Heiss WD. Ischemic penumbra: evidence from functional imaging in man. *J Cereb Blood Flow Metab* 2000; **20**:1276–1293.
22　Diaz-Arrastia R, Kochanek PM, Bergold P, Kenney K, Marx CE, Grimes CJB, et al. Pharmacotherapy of traumatic brain injury: state of the science and the road forward: report of the Department of Defense Neurotrauma Pharmacology Workgroup. *J Neurotrauma* 2014; **31**:135–158.
23　Li YH, Wang JB, Li MH, Li WB, Wang D. Quantification of brain edema and hemorrhage by MRI after experimental traumatic brain injury in rabbits predicts subsequent functional outcome. *Neurol Sci* 2012; **33**:731–740.
24　Chodobski A, Zink BJ, Szmydynger-Chodobska J. Blood–brain barrier pathophysiology in traumatic brain injury. *Transl Stroke Res* 2011; **2**:492–516.
25　Wei XE, Zhang YZ, Li YH, Li MH, Li WB. Dynamics of rabbit brain edema in focal lesion and perilesion area after traumatic brain injury: a MRI study. *J Neurotrauma* 2012; **29**:2413–2420.

26 Shlosberg D, Benifla M, Kaufer D, Friedman A. Blood–brain barrier breakdown as a therapeutic target in traumatic brain injury. *Nat Rev Neurol* 2010; **6**:393–403.

27 Galloway NR, Tong KA, Ashwal S, Oyoyo U, Obenaus A. Diffusion-weighted imaging improves outcome prediction in pediatric traumatic brain injury. *J Neurotrauma* 2008; **25**:1153–1162.

28 Hudak AM, Peng L, Marquez de la Plata C, Thottakara J, Moore C, Harper C, *et al.* Cytotoxic and vasogenic cerebral oedema in traumatic brain injury: assessment with FLAIR and DWI imaging. *Brain Inj* 2014; **28**:1602–1609.

29 Schneider G, Fries P, Wagner-Jochem D, Thome D, Laurer H, Kramann B, *et al.* Pathophysiological changes after traumatic brain injury: comparison of two experimental animal models by means of MRI. *MAGMA* 2002; **14**:233–241.

30 Albensi BC, Knoblach SM, Chew BG, O'Reilly MP, Faden AI, Pekar JJ. Diffusion and high resolution MRI of traumatic brain injury in rats: time course and correlation with histology. *Exp Neurol* 2000; **162**:61–72.

31 Marmarou A, Signoretti S, Fatouros PP, Portella G, Aygok GA, Bullock MR. Predominance of cellular edema in traumatic brain swelling in patients with severe head injuries. *J Neurosurg* 2006; **104**:720–730.

32 Kleindienst A, Dunbar JG, Glisson R, Marmarou A. The role of vasopressin V1A receptors in cytotoxic brain edema formation following brain injury. *Acta Neurochir (Wien)* 2013; **155**:151–164.

33 Maeda T, Katayama Y, Kawamata T, Koyama S, Sasaki J. Ultra-early study of edema formation in cerebral contusion using diffusion MRI and ADC mapping. *Acta Neurochir Suppl* 2003; **86**:329–331.

34 Newcombe VFJ, Williams GB, Outtrim JG, Chatfield D, Abate MG, Geeraerts T, *et al.* Microstructural basis of contusion expansion in traumatic brain injury: insights from diffusion tensor imaging. *J Cereb Blood Flow Metab* 2013; **33**:855–862.

35 Shen Q, Ren H, Cheng H, Fisher M, Duong TQ. Functional, perfusion and diffusion MRI of acute focal ischemic brain injury. *J Cereb Blood Flow Metab* 2005; **25**:1265–1279.

36 Stoffel M, Blau C, Reinl H, Breidt J, Gersonde K, Baethmann A, *et al.* Identification of brain tissue necrosis by MRI: validation by histomorphometry. *J Neurotrauma* 2004; **21**:733–740.

37 Suh DY, Davis PC, Hopkins KL, Fajman NN, Mapstone TB. Nonaccidental pediatric head injury: diffusion-weighted imaging findings. *Neurosurgery* 2001; **49**:309–318; discussion 318–320.